Delta-Sleep-Inducing Peptide: Solution Conformational Studies of a Membrane-Permeable Peptide†

Ronda A. Gray,*,‡ David G. Vander Velde,‡ Carl J. Burke,§ Mark C. Manning,∥ C. Russell Middaugh,§ and Ronald T. Borchardt‡

Department of Pharmaceutical Chemistry, University of Kansas, Lawrence, Kansas, 66045, School of Pharmacy, University of Colorado Health Sciences Center, Denver, Colorado, 80262, and Pharmaceutical Biophysics Group, Merck Research Laboratories, West Point, Pennsylvania, 19486

Received August 6, 1993; Revised Manuscript Received November 3, 1993⊛

ABSTRACT: Peptides and peptide-like molecules as a class have very poor permeability through biological membranes, which severely compromises their potential effectiveness as therapeutic agents. In order to gain insight into the problem of delivering peptide and protein drugs and to establish a model in which the effects of systematic structural variations on transport can be explored, an investigation of the solution conformation of a membrane-permeable peptide was undertaken. Delta-sleep-inducing peptide (DSIP, MW 849) was used in this investigation. DSIP is a charged, hydrophilic peptide that possesses the unusual ability to diffuse passively across the blood–brain barrier (BBB) *in vivo* [Kastin, A. J., Banks, W. A., Castellanos, P. F., Nissen, C., & Coy, D. H. (1982) *Pharmacol. Biochem. Behav. 17*, 1187–1191] and across monolayers of brain microvessel endothelial cells *in vitro*, a model of the BBB [Raeissi, S., & Audus, K. L. (1989) *J. Pharm. Pharmacol. 41*, 848–852]. This nonapeptide was studied in solution using one- and two-dimensional nuclear magnetic resonance (NMR), circular dichroism (CD), Fourier transform infrared (FT-IR), and fluorescence spectroscopies in conjunction with molecular modeling. Our spectroscopic findings suggest that DSIP exists in a dynamic equilibrium between unordered and folded structures. Residues 2–5 and 6–9 tend to form type I β-turns in aqueous solution and a similar, but more ordered, helix-like structure inducible in 40% trifluoroethanol (TFE). NMR, FT-IR, and CD studies in aqueous solution support the dynamic equilibrium hypothesis with the IR data, suggesting that the β-turn population is approximately 40%. A Trp^1 fluorescence maximum of 360 nm at pH 6.5 indicates that the indole ring is exposed to the solvent and not protected by the proposed folded structure. The fluorescence lifetime of Trp^1 also suggests that the indole ring in DSIP experiences an environment similar to that of free Trp in aqueous solution. The most ordered structure consistent with these data was one in which both proposed turns were of the βI type. This model has a compact structure with several intramolecular hydrogen bonds and appears to be amphiphilic. The structure in 40% TFE suggested by NMR and CD studies was also examined by modeling. The helix-like model that fit the TFE data was very closely related to the structure in aqueous solution (energy difference = 2.5 kcal/mol). These studies suggest that compact structures that maximize intramolecular hydrogen bonding in aqueous solution may influence permeability due to the nature of the folded structure itself or that the folded structure is an energetically favorable precursor to the preferentially permeable conformation.

It is now accepted that small peptides are able to exist in dynamic equilibria between unfolded/extended structures and ordered secondary structures before thought to be found only in larger polypeptides (Dyson et al., 1988a,b). The importance of these ordered structures has been recognized in relation to immunogenicity (Dyson et al., 1988a,b) as well as binding to receptors. Because peptide drugs are commonly plagued by delivery and/or bioavailability problems, it is also important to consider the possibility that certain conformations might permit a peptide to enter and cross a lipid membrane more readily than others.

Common molecular attributes associated with a molecule that favor permeability include decreased molecular size (Davis, 1986; McMartin & Peters, 1986), reduced charge (Humphrey, 1986), increased lipophilicity (Rosenberg et al., 1991; Cefalu & Partridge, 1985; Kleinert et al., 1992), and increased potential to form intramolecular hydrogen bonds (Conradi et al., 1991, 1992; Burton et al., 1991). Therefore, a significantly populated conformation that allows the optimization of these fundamental factors may facilitate permeability.

In this work, we discuss the presence of secondary structure in a peptide reported to possess the ability to permeate membranes, with the intent of using it and its analogs in future work as a model system with which to test the hypothesis that the presence of secondary structure in peptides affects their membrane permeability. This peptide is the delta-sleep-inducing peptide (DSIP[1]). DSIP (WAGGDASGE, M_r = 849) is an endogenous nonapeptide that is proposed to alter the sleep patterns of mammals (Graf et al., 1986) and is of interest because it has been reported to cross the blood–brain barrier (BBB) in small amounts (Kastin et al., 1979, 1981)

† This work was supported by a National Institutes of Health Predoctoral Training Grant (GM08351) in conjunction with Merck & Co. Research Laboratories (R.A.G.).

* Author to whom correspondence should be addressed. Present address: Protein Formulations, R. W. Johnson Pharmaceutical Research Institute, Route 202, P.O. Box 300, Raritan, NJ 08869.

‡ Department of Pharmaceutical Chemistry, University of Kansas.

§ Pharmaceutical Biophysics Group, Merck Research Laboratories.

∥ School of Pharmacy, University of Colorado Health Sciences Center.

⊛ Abstract published in *Advance ACS Abstracts,* January 15, 1994.

0006-2960/94/0433-1323$04.50/0

by passive mechanisms both *in vivo* (Zlokovic et al., 1989) and *in vitro* (Raeissi & Audus, 1989). The ability of this peptide to cross the BBB is quite unusual in that it possesses a net negative charge and a highly unfavorable octanol/water partition coefficient (Banks et al., 1986).

Previous rudimentary experiments and theoretical studies suggest that DSIP may exist in a semicircular or pseudocyclic conformation that allows the side chains of the C- and N-terminal residues to be close to each other in space (Mikhaleva et al., 1982; Nabiev et al., 1982). The polar side chains of Asp^5, Ser^7, and Glu^9 were proposed to be arranged such that they are folded into the interior of the looped structure, imparting a very lipophilic exterior surface to the folded structure. In this work, we use a combination of one- and two-dimensional NMR with molecular modeling, FT-IR, CD, and fluorescence techniques to propose an alternative solution structure for DSIP.

MATERIALS AND METHODS

Sample Purification. DSIP was either purchased (Peninsula Laboratories, Belmont, CA) or synthesized by solid-phase methods employing an Applied Biosystems Model 430A peptide synthesizer using Fmoc technology. All samples were purified by RP-HPLC using a Vydac 218-TP510, C-18 semipreparative column (10 mm i.d. × 25 cm long, 5 μm) and an aqueous/acetonitrile mobile phase with 0.05% TFA unless otherwise noted.

Nuclear Magnetic Resonance Spectroscopy. Three samples of DSIP were prepared for NMR experiments. Twenty milligrams of purified DSIP was dissolved in water buffered to a pH of 6.3 with 20 mM phosphate solution. This sample was lyophilized, and a 500-μL solution of the peptide in 90% water (20 mM phosphate buffer)/10% D_2O (Sigma, purity 99.9 atom % D) was prepared. For a second experiment, 20 mg of purified DSIP was prepared in 250 μL of CD_3OH/250 μL of 20 mM phosphate buffer/100 μL of D_2O. A third sample was prepared in 40% 2,2,2-trifluoroethanol-d_3 (Cambridge Isotope Laboratories)/60% 20 mM phosphate buffer.

All NMR spectra were collected at 500.13 MHz (^1H) on a Bruker AM-500 spectrometer with an Aspect 3000 computer for processing. Probe temperature calibrations were performed with a methanol standard, and all spectra were referenced to sodium 3-(trimethylsilyl)propionate-*2,2,3,3-d*$_4$ (TSP). Spectra of DSIP in 90% 20 mM phosphate buffer (pH 6.3)/10% D_2O and 58% 20 mM phosphate buffer + D_2O/42% CD_3OH were acquired at 283 K, and the spectrum in 60% 20 mM phosphate buffer/40% trifluoroethanol was obtained at 284 K. In all cases, water was suppressed by presaturation at the appropriate frequency. Plots of temperature (279–318 K) vs peak position (ppm) for each of the amide protons were made for temperature coefficient determinations. The $^3J_{N\alpha}$ values (±0.3 Hz) were determined from the amide signals of DSIP in the 1D spectra over the temperature range of 278–318 K (every 5 K). These $^3J_{N\alpha}$ values did not vary significantly with temperature. The $^3J_{N\alpha}$ values reported below are for 283 K except where noted. The two-dimensional scalar-correlated (COSY) experiments were double-quantum-filtered and were phase-sensitive (TPPI) (Rance et al., 1983). The ROESY experiments (Bothner-By et al., 1984) were also phase-sensitive and were performed with a 2-kHz spin-locking field at mixing times of 150, 200, and 300 ms. The transmitter and decoupler were phase-coherent, such that optimal water suppression could be obtained. The HOHAHA (Bax & Davis, 1985; Bax, 1989) experiments were performed with a 10-kHz spin lock at a mixing time of 70 ms using an MLEV-17 sequence with 2.5-ms trim pulses. For all 2D spectra, 2K points in f_2 and 300–512 points in f_1 were acquired with a sweep width of 6024 Hz. Processing was performed with a 90° phase-shifted, squared-sine-bell apodization function in both dimensions.

Infrared Spectroscopy. A 2-mg sample of RP-HPLC-purified DSIP was dissolved in 200 μL of D_2O (99.9%) to give a solution of pH* 3.3. A second RP-HPLC-purified sample of DSIP was dissolved, and the pH* was adjusted to 6.35 with sodium deuteroxide. A third sample of DSIP that did not undergo RP-HPLC purification was prepared similarly in D_2O (final pH* of 3.3). The samples were loaded into a CaF_2 infrared cell with a 0.1-mm path length. IR spectra were recorded with a nitrogen-flushed Bio-Rad Digilab Division FTS-60 Fourier transform spectrometer at 2-cm^{-1} resolution. The raw data were subjected to Fourier self-deconvolution, and second derivative spectra were obtained. Spectral contributions from residual water vapor were subtracted. Fourier self-deconvolution was performed using the parameters $K = 1.6$ and $\sigma = 15.5$ (Kauppinen et al., 1981). The amide I region (1600–1700 cm^{-1}) was curve-fit to a mixed Gaussian/Lorentzian function by a nonlinear least-squares program using the second derivative peak positions as initial estimates.

Circular Dichroism. CD spectra were recorded with an Aviv 62 DS spectropolarimeter at 5 and 60 °C. Peptide concentrations were determined spectrophotometrically at 280 nm. Samples of DSIP were prepared in 20 mM phosphate buffer (pH 6.5) and several compositions (0–70% (v/v) trifluoroethanol, at 10% intervals) of 20 mM phosphate buffer and trifluoroethanol (TFE, 99.5+%, Aldrich Chemical Co.). A 0.2-cm path length cell was used in all measurements. Each spectrum is the average of three individual scans, with averaging times of 3 s from 200 to 260 nm and 10 s from 186 to 200 nm in 0.5-nm intervals. Each spectrum was corrected for sample cell and solvent contributions and was smoothed with a third-order polynomial function. The difference spectra (inset, Figure 4) were obtained by subtracting the spectrum of the sample in pure phosphate buffer from the spectrum of the sample in the indicated buffer/TFE mixture.

Fluorescence. Fluorescence spectra were obtained with an SLM-8000c spectrofluorometer at both 5 and 60 °C. An excitation wavelength of 280 nm was employed, and emission was examined from 290 to 450 nm. DSIP samples were prepared at a concentration of 2.8×10^{-5} M in 20 mM phosphate buffer (pH 6.5). Fluorescence lifetime measurements were performed with a multifrequency cross-correlation phase and modulation ISS GREG fluorometer equipped with a 300-W xenon arc lamp. The peptide absorbance at 280 nm was 0.3 in 20 mM phosphate buffer. The excitation wavelength was 290 nm, and the reference used was *p*-terphenyl in absolute ethanol ($\tau = 1.05$ ns). The emission was observed through a WG 345 cut-on filter at modulation frequencies from 30 to 130 MHz (every 10 MHz) until the standard deviation from

[1] Abbreviations: DSIP, delta-sleep-inducing peptide; BBB, blood–brain barrier; NMR, nuclear magnetic resonance; NOE, nuclear Overhauser enhancement; COSY, two-dimensional *J*-correlated spectroscopy; HOHAHA, two-dimensional homonuclear Hartmann–Hahn spectroscopy; ROESY, two-dimensional rotating-frame NOE experiment; ROE, rotating-frame NOE; $^3J_{N\alpha}$, amide–α-carbon scalar coupling constant; d_{NN}, amide–amide proton distance; $d_{N\alpha}$, α-carbon–amide proton distance; CD, circular dichroism spectroscopy; FT-IR, Fourier transform infrared spectroscopy; pH*, pH uncorrected for the presence of deuterium; TFE, trifluoroethanol; TFA, trifluoroacetic acid.

Table 1: ^{1}H Assignments for DSIP[f]

residue	NH[a-c]	CHα[a-c]	CHβ[a-c]	CHγ[a-c]	ring H[a-c]
Trp[1]		4.30 (4.30, 4.35)	3.41 (3.40, 3.42) 3.41 (3.40, 3.42)[d]		HD1: 7.50 (7.35, 7.37) HE3: 7.72 (7.65, 7.70) HZ3: 7.15 (7.19, 7.21) HH2: 7.25 (7.25, 7.29) HZ2: 7.62 (7.50, 7.54) HE1: 10.32 (10.45, 10.25)
Ala[2]	8.60 (8.60, 8.64)	4.30 (4.30, 4.35)	1.28 (1.35, 1.38)		
Gly[3]	7.80 (7.70, 7.61)	3.68 (3.70, 3.76) 3.78 (3.80, 3.85)[d]			
Gly[4]	8.25 (8.20, 8.14)	3.90 (3.90, 3.97)			
Asp[5]	8.35 (8.31, 8.36)	4.59 (4.60, 4.76)	2.50 (2.71, 2.85) 2.59 (2.71, 2.93)[d]		
Ala[6]	8.42 (8.42, 8.40)	4.33 (4.32, 4.35)	1.35 (1.40, 1.44)		
Ser[7]	8.40 (8.40, 8.25)	4.35 (4.34, 4.40)	3.88 (3.90, 3.92)		
Gly[8]	8.38 (8.35, 8.28)	3.95 (3.95, 3.97)			
Glu[9]	7.90 (7.89, 7.97)	4.05 (4.12, 4.37)	β(R) 1.84 (1.85, 1.97) β(S) 2.00 (2.03, 2.19)[d]	2.16 (2.25, 2.43)	

[a] Proton assignments are based on the connectivities observed in the COSY and ROESY spectra in 90% 20 mM phosphate buffer/10% D_2O, pH* 6.5 at 283 K. [b] In 58% 20 mM phosphate buffer/42% CD_3OH-d_3 at 283 K. [c] In 60% 20 mM phosphate buffer/40% TFE-d_3 at 284 K. [d] α′ and β′ values. [e] Not observed in any of the spectra. [f] All chemical shifts are cited as ppm downfield from TSP.

each phase and modulation measurement was less than 0.600 and 0.006, respectively.

Molecular Modeling. A Silicon Graphics Personal Iris 4D25 was used to generate an idealized model of the folded structure. The software employed was QUANTA (Polygen)/CHARMM (CHARMM parameter set 22). Because no homology exists between DSIP and sequences found in the Brookhaven Protein Data Bank, the initial structure was constructed by choosing combinations of extended (ϕ,ψ for residues 1, 2, 5, 6, and 9) and β-turn conformations that were available in the software package. The eight backbone dihedral angle values (ϕ,ψ for residues 3, 4, 7, and 8) representing β-turn structure were used as constraints for the model. DSIP was generated as a zwitterion with the side chains of residues 5 and 9 in the carboxylate form. The charge of the molecule was designed to simulate the spectroscopic studies, most of which were undertaken at pH 6.5. Although the model is essentially idealized due to the constraint of the (ϕ,ψ) angles that define the turn structures, 26 ROE constraints were used (Table 4) to determine whether this model was realistic in view of the NMR data. Similarly, the χ_1 angle of Glu[9] was fixed at −60°. During the *in vacuo* minimizations, the dielectric constant was allowed to vary with distance (the form of the distance dependance was $1/r$, where r is distance). Initial *in vacuo* refinements consisted of 200 steps of steepest descent minimization followed by 100 steps of conjugate gradient and several hundred steps of adopted basis Newton–Raphson (ABNR) minimization until the change in the maximum RMS derivative was less than 0.1. Solvation of the βIβI structure was performed using an 8-Å water layer, a dielectric constant of 4.0, and the minimization methods described above.

The minimized βIβI structure obtained by utilizing the aqueous/methanol ROESY data was used as a starting structure to model DSIP in TFE. The 26 ROE constraints used (Table 4) were the same as those used in the aqueous modeling study, except that the (αH Ser[7], NH Glu[9]), (NH Ala[6], $\beta H^{1,2}$ Asp[5]), and (NH Ser[7], $\beta H^{1,2}$ Ser[7]) were replaced by (NH Ala[6], NH Gly[3]), (NH Ala[6], NH Ser[7]), (NH Ala[2], $\beta H^{1,2}$ Trp[1]), and (NH Ser[7], βH Ala[6]). All (ϕ,ψ) angles were constrained to (−75°,−33°) to drive the structure to be helix-like. The χ_1 angle was still constrained to −60°, as indicated by the stereospecifically assigned β-protons of Glu[9] in TFE.

RESULTS

Nuclear Magnetic Resonance Spectroscopy. Under all three solvent conditions, DSIP has very similar chemical shifts and coupling patterns in the 1D, ROESY and COSY spectra (Table 1). Initially, unambiguous assignments of the 1D spectra were made using peak integrations of the spectra, a 2D COSY spectrum of the 90% phosphate buffer sample and the 40% methanol sample, and a HOHAHA spectrum for the 40% TFE sample. Assignments of each of the 2D ROESY spectra were made by sequence-specific procedures described in the literature (Wüthrich, 1986). From these assignments and an examination of the ROESY crosspeaks, the secondary structural features of the peptide were determined. In each of the three solvents, all eight of the expected sequential Nα crosspeaks were observed (Figures 1b and 2b). The amide–amide region of the methanol (Figure 1a) and the phosphate spectra show unambiguous crosspeaks between the amides of residues 3–4, 4–5, and 8–9. The amide–amide region of the spectrum in TFE (Figure 2a) shows additional, resolved crosspeaks between residues 2–3 and 6–7. The remaining possible amide–amide crosspeaks (5–6 and 7–8) were not observed; however, it should be noted that the amide proton signals of residues 5 and 6 and residues 7 and 8 are nearly overlapping. Twenty-six total ROEs were used to model DSIP in all solutions with some variations (see Materials and Methods for modeling). The strongest ROEs were primarily observed for intraresidue proton correlations in all cases. Values for the amide proton temperature coefficients and $^3J_{N\alpha}$ (at 283 K) in phosphate and TFE are shown in Table 2. In phosphate buffer, residues 3, 4, 5, 8, and 9 have somewhat depressed values of the temperature coefficient and residues 3, 4, and 8 have depressed $^3J_{N\alpha}$ values. In TFE, residues 3, 4, 5, 7, 8, and 9 have relatively depressed temperature coefficients and residues 4, 6, 7, and 8 have depressed $^3J_{N\alpha}$ values.

Infrared Spectroscopy. The amide I′ region of deconvoluted FT-IR spectra has been shown to be useful in determining the relative contributions of different types of secondary structure in proteins and polypeptides (Byler & Susi, 1986; Venyaminov & Kalnin, 1990a–c) due to the sensitivity of the carbonyl stretching motions in peptides and proteins to the different secondary structure types. The amide I′ regions of the FT-IR spectra of DSIP at pH* values of 3.3 and 6.4 is shown in Figure 3. At pH* 6.4, the amide I′ region consists of seven

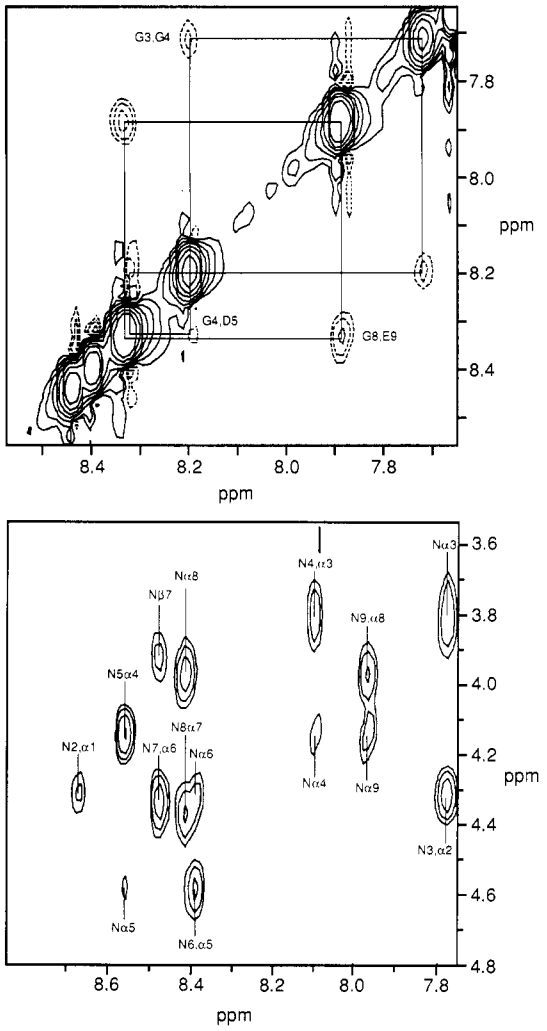

FIGURE 1: Expansions of the ROESY spectrum of DSIP in 58% 20 mM phosphate buffer/42% methanol-d_3 contours: (a, top) amide–amide region (dotted lines indicate the negative contours); (b, bottom) amide–α-carbon region.

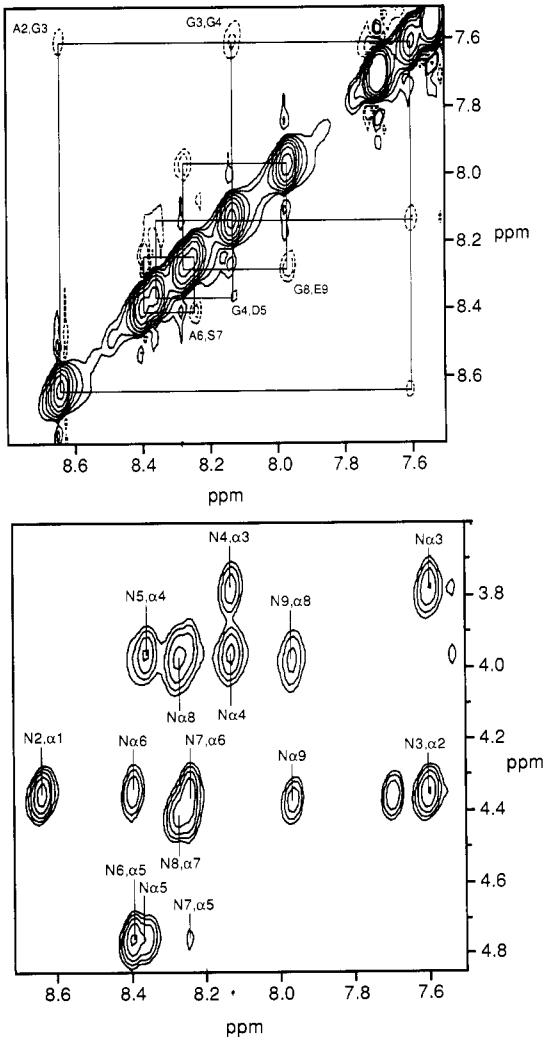

FIGURE 2: Expansions of the ROESY spectrum of DSIP in 60% 20 mM phosphate buffer/40% TFE at 284 K: (a, top) amide–amide region (dotted lines indicate the negative contours); (b, bottom) amide–α-carbon region.

bands. The lowest energy band at 1614 cm^{-1} was attributed to the N-terminus (Venyaminov & Kalnin, 1990a–c) and was not considered in the calculation of the individual contributions to the total amide I′ area. The strong band at 1673 cm^{-1} is due to contaminating trifluoroacetate (Mantsch et al., 1989) and also will not be considered further. Studies of model β-turns in the form of cyclic hexapeptides suggest that amide I′ bands between 1635 and 1650 cm^{-1} are characteristic of β-turns (Mantsch et al., 1993). Thus, the peaks at 1637 and 1648 cm^{-1} in the spectrum of DSIP, which compose 14 and 26%, respectively, of the total integrated intensity of the total relevant amide I′ peaks, are assigned to β-turn features. The presence of two distinct peaks is consistent with the existence of the proposed two β-turn-rich regions in DSIP. The peak at 1659 cm^{-1} is assigned to the nonstructural solvent-exposed carbonyl groups, while the signal at 1627 cm^{-1} has been tentatively associated with carbonyl moieties with bifurcated hydrogen bonds (Mantsch et al., 1993).

Rather similar results were obtained at pH* 3.3. In this case, only a single β-turn peak resolved at 1640 cm^{-1} composing 18% of the total integrated intensity was identified. Two peaks are present in this region that would conventionally be assigned to a non-hydrogen-bonded structure (1651 and 1661 cm^{-1}). It seems probable, however, that the 1651-cm^{-1} peak (22% of the amide I′ absorbance) is due to one of the β-turns, with its apparent frequency shift being the result of either a slightly altered environment for this turn at low pH or an artifact from a failure of the deconvolution process to accurately resolve these broad, overlapping bands. In summary, the FT-IR results suggest that approximately 40% of DSIP exists in a β-turn-rich form at both neutral and acidic pH.

Table 2: Temperature Coefficient and Coupling Constant Data for DSIP in 90% 20 mM Phosphate Buffer/10% D_2O and 60% 20 mM Phosphate Buffer/40% TFE-d_3

	temperature coefficient (ppb/K)		$^3J_{N\alpha}$ (Hz)	
residue	aqueous	TFE	aqueous	TFE
Trp[b]				
Ala[2]	7.5	8.6	6.3	5.8
Gly[3]	5.7	5.6	5.4[a]	*a*
Gly[4]	5.9	4.7	5.6, 6.3	4.7, 5.1
Asp[5]	5.6	5.8	7.2	7.1
Ala[6]	7.7	7.2	5.9[c]	5.5
Ser[7]	6.5	5.8	6.4[c]	6.4
Gly[8]	5.5	4.9	5.9	5.3, 6.1
Glu[9]	4.7	4.2	7.7	7.6

[a] Not calculated due to overlapping signals. [b] The Trp amide (N-terminus) was not observed due to rapid exchange with the solvents. [c] Determined at 278 K.

Circular Dichroism Spectroscopy. Far-UV CD spectra of DSIP in 20 mM phosphate buffer, 40% 20 mM phosphate buffer/60% TFE, and 60% 20 mM phosphate buffer/40% TFE are shown in Figure 4. In 20 mM phosphate buffer, the

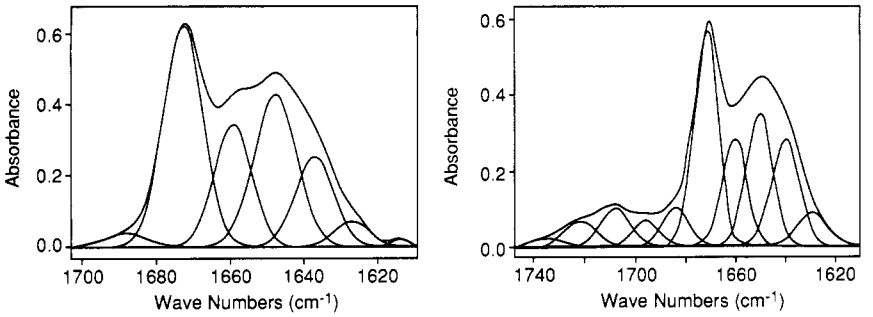

FIGURE 3: Deconvoluted amide I' region of the FT-IR spectra of DSIP in D_2O. Data were collected at (a, left) pH 6.4 and (b, right) pH 3.3.

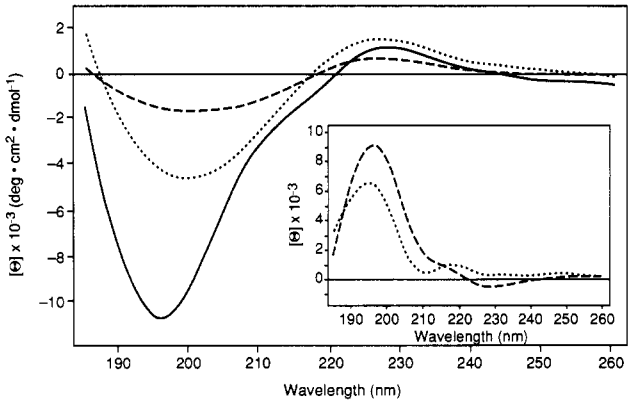

FIGURE 4: CD spectra of DSIP in 100% (—), 60% (– –), and 40% (···) 20 mM phosphate buffer with TFE. Difference spectra between the 60% and 100% spectra (– –) and the 40% and 100% spectra (···) are shown in the inset.

Table 3: Lifetime Fluorescence Parameters for DSIP in Phosphate Buffer, pH 6.5 (λ_{max} = 350 nm), at Room Temperature

	least-squares analysis	distribution analysis
χ^2	0.75	0.64
f_1	0.752	0.661
τ_1 (ns)	3.67 (W = 0.05)	3.67 (W = 0.05)
f_2	0.248	0.339
τ_2 (ns)	0.54	0.47 (W = 1.25)

two outstanding spectral features are a negative maximum at 196 nm and a positive maximum at 225 nm characteristic of disordered structure or type I β-turns (Perczel & Fasman, 1992). Upon the addition of TFE, the intensity is diminished substantially at the negative maximum and its position is shifted by 3 nm to 199 nm. The band at 196 nm appears to be more affected by TFE addition than the weaker signal at 225 nm. The main features of the buffer/TFE difference spectra (inset, Figure 4) show maxima at 196 nm for the 70% TFE sample and 198 nm for the 40% TFE sample, which are suggestive of type II β-turns (Perczel & Fasman, 1992).

Fluorescence Spectroscopy. The presence of a single Trp residue at the N-terminus of the peptide allowed intrinsic fluorescence emission spectra to be obtained at 5 and 60 °C (Table 3). The major emission feature in the 290-450-nm range at 5 °C is the presence of a single peak at 350 nm, which shifts to 356 nm.

Fluorescence lifetime data were also obtained and examined by least-squares and lifetime distribution analyses (Table 3). The phase and modulation data for DSIP were best fit (χ^2 = 0.75) to a two-component least-squares model. The major component (f_1 = 0.752) had a lifetime of 3.67 ns and the secondary component (f_2 = 0.248) a lifetime of 0.54 ns. The lifetime distribution analysis gave similar results in that a two-component model (χ^2 = 0.64) best described the data. The center of the distribution for the major contributor (f_1 = 0.661) was determined to be 3.67 ns, with a remarkably narrow distribution width of 0.05 ns. The minor component (f_2 = 0.339) had a distribution width of 1.25 ns and was centered at 0.47 ns.

Molecular Modeling Using the Aqueous and/or Methanol Data. The spectroscopic data indicate the existence of two regions in DSIP that contain β-turn structure. Although the turns are not necessarily present simultaneously in aqueous solution, the conformations most likely to favor passive transmembrane diffusion would be compact, with a maximum number of intramolecular hydrogen bonds. Accordingly, models containing various turns consistent with the data were built and energy-minimized. The ROEs used in the modeling are shown in Table 4.

The βIβI model (Figure 5) is representative and appears to fit the NMR data. The final (φ,ψ) values for residues 3–4 and 7–8 of the βIβI model were (ϕ_3 = –60.6°, ψ_3 = –30.3°, ϕ_4 = –91.1°, ψ_4 = 0.4°) and (ϕ_7 = –59.9°, ψ_7 = 29.7°, ϕ_8 = –89.0°, ψ_8 = 0.8°). This model is compact (17-Å molecular diameter) and has five intramolecular hydrogen bonds (see Table 5), consistent with the temperature coefficient data, and potential amphiphilicity is observed between the C- and N-terminal faces of this molecule (Figure 6). The Trp ring is surface-exposed, as indicated by the fluorescence studies, on the N-terminal face.

Additional support for this model was shown by an independent modeling study in which DSIP was constructed as an extended structure. Only the three d_{NN} ROE constraints were applied. The structure that resulted from minimization exhibited (φ,ψ) angles for residues 3–4 and 7–8 at (ϕ_3 = –53°, ψ_3 = 38°, ϕ_4 = –92°, ψ_4 = 44°) and (ϕ_7 = –55°, ψ_7 = 28°, ϕ_8 = –100°, ψ_8 = 17°), respectively.

Molecular Modeling Using the TFE Data. A helix-like model representing the structure of DSIP in TFE is shown in Figure 7. Following energy minimization, this model had all dihedral angles of ϕ = –75 ± 5°, ψ = –33 ± 5°. The net minimized energy was only slightly lower (2.5 kcal/mol) than that of the minimized βIβI structure. The energy term that gained the most stabilization in converting the βIβI structure to a helical form was the dihedral angle term. All of the ROE constraints were satisfied by this model, which exhibited five hydrogen bonds (see Table 5).

DISCUSSION

Although the averaging of conformations on the time scale of the NMR experiments occurs with short linear peptides, several NMR criteria have been reported to be sufficient to characterize molecules with populations of β-turns (Dyson & Wright, 1991). These include decreased amide signal temperature coefficients (for the amides involved in intramolecular

Table 4: ROE Proton Correlations for DSIP in Aqueous[a] and TFE[b] Solutions

ROE strength	aqueous	TFE
weak (2.0–4.5 Å)	Gly^{4}NH–Asp^{5}NH	Gly^{4}NH–Asp^{5}NH
	Ala$^2\alpha$H–Gly^{4}NH	Ala$^2\alpha$H–Gly^{4}NH
	Ser$^7\alpha$H–Glu^{9}NH	
	Ala$^6\beta$H–Ala^{6}NH	Ala$^6\beta$H–Ala^{6}NH
	Glu$^9\beta$H–Glu$^9\gamma$H,γ'H	Glu$^9\beta$H–Glu$^9\gamma$H,γ'H
	Ala$^2\beta$H–Ala^{2}NH	Ala$^2\beta$–Ala^{2}NH
		Ala^{2}NH–Gly^{3}NH
medium (2.0–3.5 Å)	Gly^{8}NH–Glu^{9}NH	Gly^{8}NH–Glu^{9}NH
	Gly^{3}NH–Gly^{4}NH	Gly^{3}NH–Gly^{4}NH
	Ala^{6}NH–Asp$^5\beta$H,β'H	
	Asp^{5}NH–Asp$^5\beta$H,β'H	Asp^{5}NH–Asp$^5\beta$H,β'H
	HD(1)–β,β'1	HD(1)1–β,β'1
	HE(3)1–β,β'1	HE(3)1–β,β'1
	Ser^{7}NH–Ser$^7\beta$-,β'H	
		Ala^{6}NH–Ser^{7}NH
		Ala^{2}NH–Trp$^1\beta$H,β'H
		Ser^{7}NH–Ala$^6\beta$H
strong (2.0–3.0 Å)	Glu$^9\beta(R)$H–Glu^{9}NH	Glu$^9\beta(R)$H–Glu^{9}NH
	Glu^{9}NH–Glu$^9\gamma$H,γ'H	Glu^{9}NH–Glu$^9\gamma$H,γ'H
	Glu$^9\alpha$H–Glu$^9\gamma$H,γ'H	Glu$^9\alpha$H–Glu$^9\gamma$H,γ'H
	Glu$^9\alpha$H–Glu$^9\beta(R)$H,$\beta(S)$H	Glu$^9\alpha$H–Glu$^9\beta(R)$H,$\beta(S)$H

[a] Aqueous data are from the 300-ms ROESY in 90% 20 mM phosphate buffer/10% D_2O. [b] TFE data are from the ROESY in 60% 20 mM phosphate buffer/40% TFE-d_3.

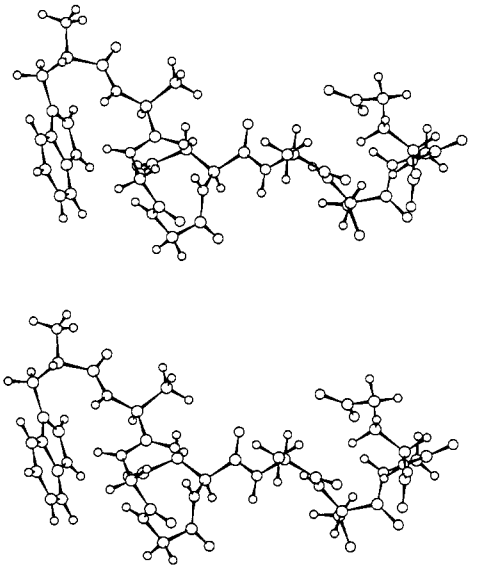

FIGURE 5: Minimized molecular model of a significantly populated folded structure of DSIP in aqueous solution. The intramolecular hydrogen bonds corresponding to this model are found in Table 5.

Table 5: Intramolecular Hydrogen Bonds Suggested from Molecular Modeling of DSIP[a]

	H donor	H acceptor	distance (Å)	angle (deg,N–H···O)
A	NH 4	CO 1	1.98	138.3
	NH 5	CO 2	1.92	162.6
	NH 8	COO 5	2.00	140.0
	NH 5	CO 1	2.61	91.0
	NH 9	CO 6	2.03	163.9
B	N-terminal H	COO 5	2.30	154.5
	NH 4	CO 1	2.70	136.4
	NH 5	CO 2	2.50	141.5
	NH 8	COO 5	2.10	130.3
	NH 9	CO 6	2.20	134.6

[a] Constraints were derived from the NMR data in aqueous (A) and TFE (B) solvents.

hydrogen bonds), decreased $^3J_{N\alpha}$ coupling constants for the center residues, and characteristic NOE connectivities best observed for molecules of this size via ROESY experiments. For example, the observation of several characteristic peaks in a ROESY spectrum can aid in the identification of a β-turn. These characteristic peaks include a $d_{NN}(3,4)$ ROE, a weaker $d_{\alpha N}(2,4)$ ROE, and possibly a $d_{NN}(2,3)$ ROE, indicating a βI-turn structure, or a $d_{\alpha N}(2,3)$ ROE, suggesting the presence of a βII-turn.

In general, glycine residues are favored for steric reasons in β-turns, particularly in the $i + 2$ position, and can act as a virtual L- or D-amino acid in any of the four most commonly observed turn types (I, I′, II, and II′). The dipeptide sequences Ala-Gly and Ser-Gly, found in DSIP, frequently occur in protein structures at the center of turns (Smith & Pease, 1980). The Gly-Gly sequence is also a potential turn center. Consequently, it is not surprising that the ROESY spectra of DSIP in phosphate buffer and methanol/phosphate buffer each exhibit several of the significant crosspeaks characteristic of β-turns. Observation of the d_{NN}(Gly^3,Gly^4) and d_{NN}(Gly^4,Asp^5) crosspeaks could suggest the following: (1) Residues 2–5 define the first turn, with Asp^5 as the fourth residue of the turn; the presence of the d_{NN}(Gly^4,Asp^5) and $d_{\alpha N}$(Ala^2,Gly^4) crosspeaks support type I β-turn structure for this turn. (2) There is an equilibrium between a 2–5 turn and a 1–4 turn, where each d_{NN} observed marks residues 3 and 4 of a different turn (the type of turn, particularly for the 2–5 turn, would be difficult to distinguish). Work in progress on cyclic DSIP analogs has uncovered evidence for the 1–4 turn being favored, depending on the type of cyclization (F. Okumu, T. J. Siahaan, D. G. Vander Velde, and R. T. Borchardt, unpublished results). (3) A γ-turn comprises Ala^2–Gly^4, which is consistent with evidence from shorter fragments of DSIP (Okumu et al., unpublished results). From coupling constant data (see below), option 1 seems more likely for native DSIP; hence, the latter possibilities will not be considered further here. The observation of the d_{NN}(Gly^8,Glu^9) and $d_{\alpha N}$(Ser^7,-Glu^9) crosspeaks supports β-turn structure in residues 6–9, with Glu^9 as the fourth residue of the second turn. Significant signal overlap in the amide region prevents the observation of the possible d_{NN}(Ser^7,Gly^8) crosspeak that could aid in the assignment of the type of turn. However, the d_{NN}(Val^7,Gly^8) crosspeak [as well as the d_{NN}(Gly^3,Gly^4) and d_{NN}(Gly^8,Glu^9)] of a Val^7 analog of DSIP is observed (R. A. Gray, D. G. Vander Velde, C. J. Burke, M. C. Manning, C. R. Middaugh, and R. T. Borchardt, unpublished results). This analog has

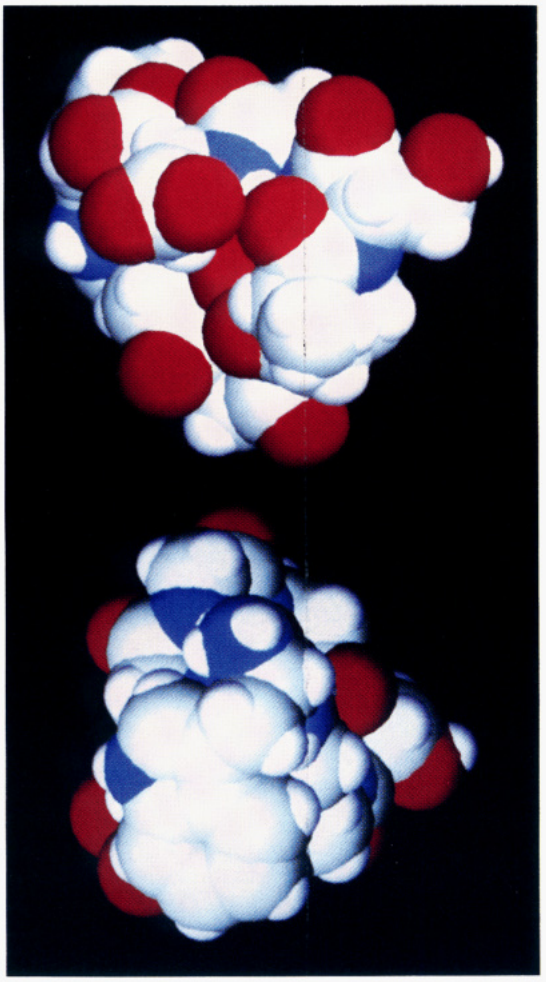

FIGURE 6: Space-filling model of DSIP in aqueous solution as viewed from (a, top) the C-terminal face of the molecule, which exhibits a clustering of polar groups, especially oxygens (shown in red), and (b, bottom) the N-terminal face, which shows more lipophilic groups and the N-terminus.

been determined to have a conformation very similar to that of DSIP itself, despite the change in the primary sequence (Gray et al., unpublished results). Because the two peptides are believed to have very similar structures, observation of the d_{NN}(Val^7,Gly^8) crosspeak provides further support for the second turn to be a type I β-turn.

The observation of increased signal dispersion and additional unambiguous sequential amide–amide ROE correlations in the spectrum of DSIP in 40% TFE support the existence of a more ordered, helix-like structure. Specifically, the d_{NN}(2,3) and d_{NN}(6,7) crosspeaks were observed in the spectrum in TFE that were not found in the aqueous and aqueous/methanol spectra. Observation of five (again, the other two possible correlations, if present, could not be seen because the diagonal signals were nearly overlapping) of the eight possible amide–amide ROEs, as opposed to three of the eight, supports the existence of a more ordered, helix-like structure. Thus, it appears that the βIβI form may be the stable structure in aqueous solution and that it is a precursor that is easily converted to a helix-like conformation in the presence of a structure-promoting environment. This is not surprising since the angles defining type I β-turns are similar to those defining helices (Perczel et al., 1991). The five potential hydrogen bonds suggested by the variable-temperature NMR studies are supported nicely by this model, as is the unique difference CD spectrum shown in Figure 4.

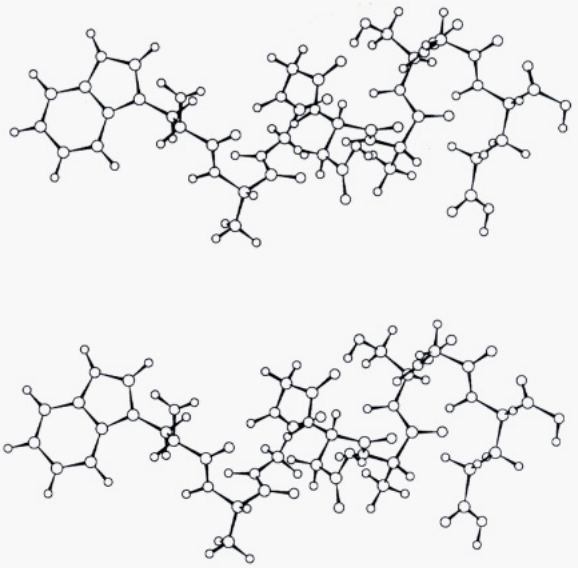

FIGURE 7: Minimized molecular model of a significantly populated folded structure of DSIP in TFE/aqueous solution. The intramolecular hydrogen bonds corresponding to this model are found in Table 5.

The presence of a backbone amide proton to carbonyl oxygen hydrogen bond from the fourth residue of a turn to the first residue in a β-turn is also useful in identifying a β-turn. The amide proton temperature coefficients in phosphate buffer were determined, and several of these coefficients were found to be relatively low. This indicates that a structure in which these protons are protected from solvent exchange by hydrogen bonding is likely. Two of these depressed values were found for the amide protons of residues 5 and 9 (Table 2). Considering the turn positions of these residues suggested by the ROE data (residues 5 and 9 were proposed as the fourth residue of each turn) and the fact that the temperature coefficient values indicate that these amide protons are protected from exchange to some degree, it is possible to conclude that potential sites for intramolecular hydrogen bonding exist between the carbonyl oxygen of residue 2 and the amide proton of residue 5 and between the carbonyl oxygen of residue 6 and the amide proton of residue 9. The existence of these hydrogen bonds is further supported by the βIβI modeling in which energetically favorable hydrogen bonds are found between the indicated atoms of residues 2 and 5 and those of residues 6 and 9 (Table 5). In the helix-like model, all amide residues greater than residue 4 (residue 4 included) should be hydrogen-bonded; residue 6 was found to be the only exception.

In order to investigate the possibility that the side chain of Glu^9 may be responsible for its depressed temperture coefficient due to intramolecular hydrogen bonding, stereospecific assignments of the β-protons of Glu^9 were made by the procedure of Clore and Groenenborn (1989). The value of the χ_1 side-chain dihedral angle for this residue was determined to preferentially populate [approximately 60% population, Kobayashi et al. (1981)] the –60° conformer. This assignment is based on $^3J_{\alpha\beta}(R)$ = 9.2 Hz and $^3J_{\alpha\beta}(S)$ = 4.7 Hz and on the observation that the amide to $\beta(R)$-proton of residue 9 has a stronger ROE than the amide to $\beta(S)$-proton of the same residue. This value (χ_1 = –60°) was used to investigate the likelihood of intraresidue hydrogen bonding between the side chain of this acidic residue and its own amide proton. In this modeling study, the acidic residue's side-chain, deprotonated oxygens were constrained to be 2.0 ± 0.02 from the indicated amide proton. Complete energy minimization (RMS deriv-

ative <0.01 for 200 steps) resulted in only a very weak hydrogen bond (distance = 2.35 Å, angle = 112.1°) between the amide proton and the carboxyl side chain. Thus, even in the extreme case in which a hydrogen bond is strongly constrained, this interaction does not seem probable. Unfortunately, the stereospecific assignments of the β-protons of other residues such as Asp[5] were not possible.

Amide–α-carbon scalar coupling constant data for the second and third residues of the proposed β-turns are complementary to the ROE and temperature coefficient data. Values of $^3J_{N\alpha}$ consistent with nonfolded structures are usually on the order of 7–9 Hz, whereas values for the second and third residues in a β-turn structure typically are depressed to approximately 5 Hz (Dyson et al., 1988a; Wagner et al., 1986). Three such lowered $^3J_{N\alpha}$ values were observed. For the proposed first turn in DSIP, residues 2 and 3 (Gly[3] and Gly[4], respectively) were found to exhibit values of 5.4 and 5.6 Hz, most consistent with a turn being centered there. As noted in Table 2, these values are low relative to the other values found within the first proposed turn. Similarly, for the second proposed turn in DSIP, Gly[8] had a depressed $^3J_{N\alpha}$ value of 5.9 Hz and Ser[7] was found to have a $^3J_{N\alpha}$ of 6.4 Hz (278 K), which are low relative to the values for the remaining residues of the second turn. The results from this amide–α-carbon *J*-coupling study indicate that residues Gly[3],Gly[4] and Ser[7],Gly[8] are likely to be residues 2 and 3 of β-turns one and two, respectively, in DSIP.

The dynamic equilibrium hypothesis is further supported by the IR data of DSIP in aqueous solution at pH* 3.3 and 6.5. Analysis of the amide I′ region finds that the majority of the absorbance in this region can be assigned to turn or unfolded conformations. Although contributions from extended and unordered structures are observed, the predominant secondary structural element appears to be to β-turn structure, as suggested by the presence of two bands in the 1635–1651-cm^{-1} region (Mantsch et al., 1993). Analysis of the area under these peaks suggests that DSIP may occupy a folded conformation approximately 40% of the time. Similarities in the spectra at pH* 2 and 6 suggest that the gross conformation is not greatly altered by pH. Thus, salt bridges do not appear to be a major factor in the stabilization of the structured form of the peptide.

The shape and positions of the extrema in the CD spectrum of DSIP in 20 mM phosphate buffer are primarily representative of a disordered peptide. This is again consistent with the largest conformational population being unfolded. While the negative maximum at 196 nm arises from peptide moieties, the maximum at 225 nm probably arises from the intrinsic optical activity of the Trp residue (Adler et al., 1973). In an attempt to induce detectable structure into the peptide, TFE, which is known to impart such character, was added to the aqueous solutions of DSIP. Upon exposure of the peptide to TFE, the most dramatic change in the spectrum occurs at 196 nm, suggesting that the structure is being perturbed. The change in the 225-nm band is quite small. In order to establish the nature of the structure induced by the TFE, difference spectra (Figure 5, inset) were generated. The outstanding features in these difference spectra are the maxima at 196–197 nm.

β-Turns have traditionally been the most difficult conformations to identify unambiguously by CD (Perczel & Fasman, 1992; Perczel et al., 1991). It has been reported that the CD spectra of type I β-turns often resemble those of α-helices (Dyson & Wright, 1991), with a positive maximum observed around 196 nm and negative maxima at 208 and 222 nm. In an attempt to more definitively characterize the CD spectra of different types of β-turns, Perczel and Fasman (1992) studied a series of cyclic pseudohexapeptides by NMR/molecular dynamics and CD. The CD curves were conformationally deconvoluted using convex constraint analysis (Perczel et al., 1991) to yield the pure component CD spectra of type I and type II β-turns. The CD characteristics of the pure βI type curve had a maximum at 195 nm and negative maxima at 209 and 225 nm, while a second type of βI-turn exhibited a weaker negative maximum at 205 nm. In contrast, βII-turns manifest a positive peak near 200 nm much like that seen in the DSIP difference spectra. Thus, while a less polar solvent also seems to induce a β-turn-rich structure, a subtle difference in the nature of the turns seems implied by these results.

The results from the study of the intrinsic fluorescence of Trp[1] (λ_{max} = 350 nm in pH 6.5 aqueous solution) are in agreement with the βIβI model, which suggests that the indole ring is surface-exposed. The lifetime and lifetime center-of-distribution of the major components of the Trp fluorescence (f_1 = 0.752 and f_1 = 0.661, respectively) had values of 3.67 ns. This value suggests that the indole ring is not located in an apolar environment, since it is consistent with the value reported by Alcala (1987) for free Trp in aqueous solution (pH 6). The best fit of the discrete and distribution data to two components may reflect the sensitivity of the indole to subtly different environments as a consequence of interconverting conformations or may simply reflect the different microenvironments sampled by the indole ring because of its inherent occupation of different rotamer populations (Lakowicz, 1983; Lakowicz et al., 1983, 1984).

In summary, a variety of spectroscopic techniques has been employed to characterize the solution structure of DSIP. On the basis of these data and molecular modeling simulations, DSIP is suggested to exist in a dynamic equilibrium involving unfolded and folded structures (two β-turn-rich regions in water and a helix-like structure in TFE). On the basis of model building, these conformational features impart compactness and amphiphilicity to DSIP. Thus, the conformation of DSIP, perhaps by virtue of some combination of these contributing factors, may be responsible for its ability to cross membranes. Using what we have reported about the solution structure of DSIP, we plan to examine this hypothesis by seeking correlations between secondary structure population and membrane permeability among analogs of DSIP; other families of peptides known to have secondary structure whose type and population depend on sequence are also being actively investigated in our laboratory.

ACKNOWLEDGMENT

We acknowledge Dr. Gautam Sanyal, Mr. Mark Bruner, Ms. Dorothy Marquis-Omer, and Mr. James Ryan (Merck Research Laboratories) for their technical assistance with HPLC and the various spectroscopic techniques. We also acknowledge Professor Teruna Siahaan (University of Kansas) for helpful discussions.

REFERENCES

Adler, A. J., Greenfield, N. J., & Fasman, G. D. (1973) *Methods Enzymol. 27*, 675–735.

Alcala, J. R., Gratton, E., & Prendergast, F. G. (1987) *Biophys. J. 51*, 925–936.

Banks, W. A., Kastin, A. J., Coy, D. H., & Angulo, E. (1986) *Brain Res. Bull. 17*, 155–158.

Bax, A. (1989) *Methods Enzymol. 176*, 151–168.

Bax, A., & Davis, D. G. (1985) *J. Magn. Reson. 65*, 355–360.
Bothner-By, A. A., Stephens, R. L., Lee, J., Warren, C. D., & Jeanloz, R. W. (1984) *J. Am. Chem. Soc. 106*, 811–813.
Burton, P. S., Conradi, R. A., & Hilgers, A. R. (1991) *Adv. Drug Deliv. Rev. 7*, 365–386.
Byler, D. M., & Susi, H. (1986) *Biopolymers 25*, 469–487.
Cefalu, W. T., & Pardridge, W. M. (1985) *J. Neurochem. 45* (6), 1954–1956.
Clore, G. M., & Gronenborn, A. M. (1989) *CRC Crit. Rev. Biochem. Mol. Biol. 24* (5), 479–564.
Conradi, R. A., Hilgers, A. R., Ho, N. F. H., & Burton, P. S. (1991) *Pharm. Res. 8* (12), 1453–1460.
Conradi, R. A., Hilgers, A. R., Ho, N. F. H., & Burton, P. S. (1992) *Pharm. Res. 9* (3), 435–439.
Davis, S. S. (1986) in *Delivery Systems for Peptide Drugs* (Davis, S., Illum, L., & Tomlinson, E., Eds.) pp 1–21, Plenum Press, New York.
Dyson, H. J., & Wright, P. E. (1991) *Annu. Rev. Biophys. Biophys. Chem. 20*, 519–538.
Dyson, H. J., Rance, M., Houghten, R. A., Lerner, R. A., & Wright, P. E. (1988a) *J. Mol. Biol. 201*, 161–200.
Dyson, H. J., Rance, M., Houghten, R. A., Wright, P. E., & Lerner, R. A. (1988b) *J. Mol. Biol. 201*, 201–217.
Graf, M. V., & Kastin, A. J. (1986) *Peptides 7*, 1165–1187.
Humphrey, M. J. (1986) in *Delivery Systems for Peptide Drugs* (Davis, S., Illum, L., & Tomlinson, E., Eds.) pp 139–151, Plenum Press, New York.
Kastin, A. J., Nissen, C., Schally, A. V., & Coy, D. H. (1979) *Pharmacol. Biochem. Behav. 11*, 717–719.
Kastin, A. J., Nissen, C., & Coy, D. H. (1981) *Pharmacol. Biochem. Behav. 15*, 955–959.
Kastin, A. J., Banks, W. A., Castellanos, P. F., Nissen, C., & Coy, D. H. (1982) *Pharmacol. Biochem. Behav. 17*, 1187–1191.
Kauppinen, J. K., Moffatt, D. J., Mantsch, H. H., & Cameron, D. G. (1981) *Anal. Chem. 53*, 1454–1457.
Kleinert, H. D., Rosenberg, S. H., Baker, W. R., Stein, H. H., Klinghofer, V., Barlow, J., Spina, K., Polakowski, J., Kovar, P., Cohen, J., & Denissen, J. (1992) *Science 257*, 1940–1943.
Kobayashu, J., Higashijima, T., Sekido, S., & Miyazawa, T. (1981) *Int. J. Pept. Protein Res. 17*, 486–494.
Lackowicz, J. R., Maliwal, B. P., Cherek, H., & Balter, A. (1983) *Biochemistry 22* (8), 1741–1752.
Lackowicz, J. R., Laczko, G., Cherek, H., Gratton, E., & Limkeman, M. (1984) *Biophys. J. 46*, 463–477.
Levitt, M., & Perutz, M. F. (1988) *J. Mol. Biol. 201*, 751–754.
Mantsch, H. H., Surewicz, W. K., Muga, A., Moffatt, D. J., & Casal, H. L. (1989) *SPIE Annu. Tech. Symp. Proc. 1145*, 580–581.
Mantsch, H. H., Perczel, A., Hollosi, M., & Fasman, G. D. (1993) *Biopolymers 33*, 201–207.
McMartin, C., & Peters, G. (1986) in *Delivery Systems for Peptide Drugs* (Davis, S., Illum, L., & Tomlinson, E., Eds.) pp 255–263, Plenum Press, New York.
Mikhaleva, I., Sargsyan, A., Balashova, T., & Ivanov, V. (1982) in *Chemistry of Peptides and Proteins, Volume 1* (Voelter, W., Byer, E., Ovchinnikov, Y. A., & Ivanov, V. T., Eds.) pp 289–297, Walter de Gruyer & Co., Berlin.
Nabiev, I. R., Sargysan, A. S., Efremov, E. S., Mikhaleva, I. I., & Ivanov, V. T. (1982) *Bioorg. Khim. 8*, 900–904.
Perczel, A., & Fasman, G. D. (1992) *Protein Sci. 1*, 378–395.
Perczel, A., Hollosi, M., Foxman, B. M., & Fasman, G. D. (1991) *J. Am. Chem. Soc. 113*, 9772–9784.
Raeissi, S., & Audus, K. L. (1989) *J. Pharm. Pharmacol. 41*, 848–852.
Rance, M., Sorenson, O. W., Bodenhausen, G., Wagner, G., Ernst, R. R., & Wüthrich, K. (1983) *Biochem. Biophys. Res. Commun. 117*, 479–485.
Rosenberg, S. H., Kleinert, H. D., Stein, H. H., Martin, D. L., Chekal, M. A., Cohen, J., Egan, D. A., Tricarico, K. A., & Baker, W. R. (1991) *J. Med. Chem. 34*, 469–471.
Smith, J. A., & Pease, L. G. (1980) *CRC Crit. Rev. Biochem. 8* (4), 315–400.
Venyaminov, S. Y., & Kalnin, N. N. (1990a) *Biopolymers 30*, 1243–1257.
Venyaminov, S. Y., & Kalnin, N. N. (1990b) *Biopolymers 30*, 1259–1271.
Venyaminov, S. Y., & Kalnin, N. N. (1990c) *Biopolymers 30*, 1273–1280.
Wagner, G., Heuhaus, D., Worgotter, E., Vasak, M., Kagi, J. H. R., & Wüthrich, K. (1986) *J. Mol. Biol. 187*, 131–135.
Wüthrich, K. (1986) *NMR of Proteins and Nucleic Acids*, John Wiley and Sons, Inc., New York.
Zlokovic, B. V., Susic, V. T., Davson, H., Begley, D. J., Jankov, R. M., Mitrovic, D. M., & Lipovac, M. N. (1989) *Peptides 10*, 249–254.